Eletrônica de Potência
Open Journal of Power Electronics

Received April 18, 2024; accepted July 30, 2024; Date of publication August 13, 2024.
The review of this paper was arranged by Associate Editor Edivan L. C. da Silva and Editor-in-Chief Heverton A. Pereira.
Digital Object Identifier http://doi.org/10.18618/REP.2005.1.006011

Laboratory Supported Lectures on Modeling: Transformer Case

Vinicius Negri Machado[1], Fernando Ortiz Martinz[1], Wilson Komatsu[1], Lourenco Matakas Junior[1]

Polytechnic School of the University of São Paulo, Electrical Energy and Automation Department, São Paulo - SP, Brazil.

e-mail: vininegri.2000@usp.br, fernando.martinz@alumni.usp.br, wilsonk@usp.br, matakas@usp.br.

ABSTRACT The modeling process of a component or system consists of several steps, which are rarely entirely covered in undergraduate courses. Moreover, theoretical and laboratory lectures focus on different stages on modeling, and are commonly taught at different periods, which may negatively affect the learning process. Thus, this paper proposes a set of lectures that mixes theory and experiments, taught in an experimental laboratory, and which address all steps of modeling process. The case study is a single-phase transformer, where from a conceptual (electromagnetic) model, physical (electrical) models are developed up to a model capable of representing more complex phenomena such as inrush currents and magnetizing inductance saturation. Increasingly detailed theoretical modeling, using simulation tools and experimental measurements, guides the student in this process. It is shown that models can be improved at the expense of deeper understanding of the involved phenomena, and of more complex theoretical and experimental strategies to validate them. Moreover, this paper demonstrates that modeling complexity is only necessary up to a point which explains adequately the experimental results. Finally, the paper presents the perception of the students on the lectures, indicating that this teaching methodology can be adequate for other courses on system modeling.

KEYWORDS Inrush current, modeling process, power electronics laboratory, saturation, transformer models.

I. INTRODUCTION

The modeling process of a component/system is composed by the following steps [1]: i) understanding and analysis of the real system; ii) decision on the simplifying hypotheses; iii) definition of the conceptual model; iv) physical modeling of the components/system based on simplifying hypotheses; v) mathematical modeling and more simplifying hypotheses to obtain a set of equations; vi) parameters determination; vii) analytical solution or numerical simulations; viii) model validation by experiments, and ix) proposal of improvements to the model until satisfactory results are achieved in the description of the studied phenomenon. Modeling is used in all the lectures of engineering courses, but usually theoretical lectures concentrate on steps iv, v, and vii. Laboratory lectures usually focus on vi, vii and viii. However, authors believe that it is important to provide, at times during the course, the opportunity for the student to experience all the stages of modeling a phenomenon. It is a good opportunity to review and join concepts from other lectures.

In this way, the main contribution of this paper is to present a learning methodology, based on a set of lectures that mixes theory and experiments, taught in an experimental laboratory, which introduces all steps of the modeling process to undergraduate students. Five lectures of 100 minutes each on modeling - 3 on transformers, 1 on diode junction and 1 on thermal model - were included in the laboratory lectures at the beginning of a 2 semester Power Electronics (PE) course at the Electrical Energy and Automation Department of the Polytechnic School of the University of São Paulo (PEA-EPUSP). The PE course at PEA-EPUSP is divided in two parts, PE-1 and PE-2, each one with 13x100 minutes laboratory lectures and 13x100 conventional classroom lectures, with additional 5 hours dedicated to tests for evaluating students. So, the complete PE course has 96.6 hours. Of these, 43.3 hours are taught in the experimental laboratory, 43.3 are in a conventional classroom and 10 are dedicated to tests. This paper focuses on the 3 lectures about transformer modeling, but this learning methodology is extended to the whole Power Electronics course. These three modeling lectures, taught in the experimental laboratory, totalize 5 hours.

The reason for choosing the transformer is that understanding magnetics is fundamental for the students, since as stated in [2] [3] most of power electronics topologies use some form of magnetic energy storage and transformation. Furthermore, the fact that undergraduate and graduate students as well as many professionals misplace the linear models, and misuse them to explain the real transformer, led the authors to sequentially present to the students the conceptual, the ideal, the T-linear and the T-nonlinear transformer models, showing how the increasing complexity of modeling improves the ability of the model to explain the phenomena experimentally observed [4].

The transformer lectures show that models can be improved at the expense of: a) a deeper study of the phenomena; b) the use of a more complex model (which inevitably brings the need for theoretical or experimental strategies to obtain new parameters), and c) the need for model validation [5]. Additionally, the conclusion is that the best model is the simplest one that adequately describes the desired phenomena with satisfactory error.

For instance, the ideal model in used in power electronics applications, in the first steps of the modeling, to obtain simplified equations that enable the understanding of the circuit behavior and its design, such as in Switched-mode Power-supplies (Push-pull [6] [7], Half and Full bridge Converters [6] [7]).

The T-linear model is commonly adopted for short-circuit [8], load flow and stability [9], microgrid [10], power quality [11] studies, etc., in power systems. This is usually the model employed in electromechanical energy conversion undergraduate lectures [12]. In power electronics, the use of the T-linear model is necessary to explain some converter topologies, e.g. Forward and Flyback converters [6] [7] [13] and Dual Active Bridge [14].

The T-nonlinear model is necessary when the focus is on the analysis of distorted magnetization current and inrush phenomena in power transformers [15] [16], saturation of current transformers for measurement purposes [16], or on differential relays for power transformers [16]. An important use of this model is to study the effect of DC current injection in the secondary of distribution transformers caused by non-isolated, grid connected power electronics converter (e.g. renewable energy sources systems - RES) [17]. In power electronics, the T-nonlinear models can be used to evaluate the counter measures to avoid core saturation in Dynamic Voltage Restorer [18], Uninterruptible Power Supply [19], in association of Power Converters [20], etc.

Further improvements for high frequency operation, that includes the parasitic capacitances, for leakage currents and EMI studies, and improved models for copper and core losses are out of the scope of the reported lectures.

II. EXPERIMENTAL SETUP

The experimental setup (Fig. 1) employs some modules of the 'Experimental Platform for Learning Self Commutated Converters', used for the undergraduate and graduate lectures of the PEA-EPUSP [21]. It was designed and constructed by its Power Electronics Group.

The experiments use: (a) the single-phase output of a three phase AC source module (12V rms, 3A rms) with relay switched output (Fig. 1a); (b) a module containing a 6VA (12V rms -12V rms) 60Hz single phase transformer, whose secondary has a series diode that can optionally be added to implement a one-way rectifier (Fig. 1b), and (c) a load module composed by 6 x 100Ω parallel switched resistors per phase (Fig. 1c). The choice for low power is essentially the cost. The choice for low voltage is a safety directive [22]. An off-the-shelf product, purchased on the electronics market, was used.

Additional required equipment includes: i) digital oscilloscope with a sampling frequency higher than 50ksa/s, a memory depth higher than 2k samples, and 2 or more input channels (Keysight DSO1024A was used); ii) DC/AC current probe with 5A range, and bandwidth higher than 20kHz (Cybertek CPL8100A was used); iii) variable transformer; iv) software for numerical calculation (MATLAB was used); and v) software for circuit simulation (PSIM was used).

III. PROPOSED UNDERGRADUATE EXPERIMENTAL LECTURES ABOUT TRANSFORMER MODELING

The three proposed lectures have as prerequisites that the students: a) have basic Electric Circuit knowledge (sinusoidal steady state and transient operation); b) have already learned the ideal and T-linear transformer models, with the open and short circuit tests for parameter estimation; c) know how to use an oscilloscope and how to do data acquisition, including transient measurements; d) can use MATLAB (or equivalent) to post process the acquired data, and e) can use some electrical circuit simulator (such as PSPICE or PSIM). Tutorials in video and text formats are available on the Moodle platform before the start of the course. They include topics that review the necessary theory, and the use of oscilloscopes, current probes, data acquisition, etc. Authors consider that any lecture can be a great opportunity to review, consolidate and apply previously learned concepts.

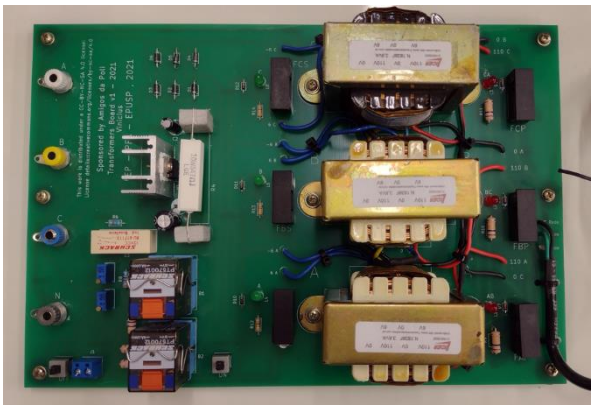

(a)- AC source module (12V rms, 3A rms).

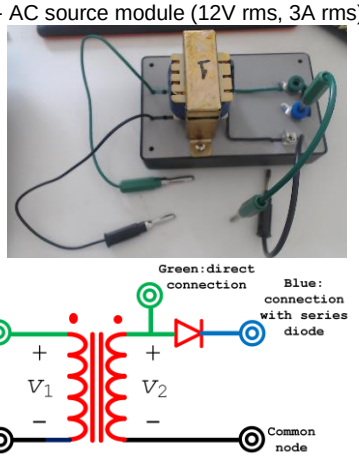

(b)- 6VA (12V-12V) single phase transformer.

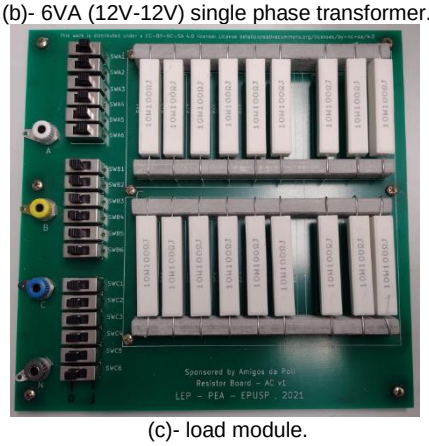

(c)- load module.

FIGURE 1. Modules used for the experiments.

This set of lectures uses MATLAB functions to process voltage and current waveforms, and to calculate their spectra, the active power, their rms values, and to plot their waveforms and spectra. Besides that, PSIM is used to simulate the transformer models for further comparison with experimental results. Below is a brief description for each of the 3 lectures.

A. *1st LECTURE: EXPERIMENTAL MEASUREMENTS AND IDEAL TRANSFORMER MODEL*

1) Description of 9 test cases to be used along the 3 lectures
   - 3 loads: a) no-load, b) resistive load, c) one-way rectifier with resistive load (See Fig. 2).
   - 3 modes of operation, for each load type: a) energizing at the instant when the sinusoidal grid voltage is zero ($\theta=0^o$); b) energizing when the grid voltage is equal to its peak value ($\theta=90^o$), and c) steady state.

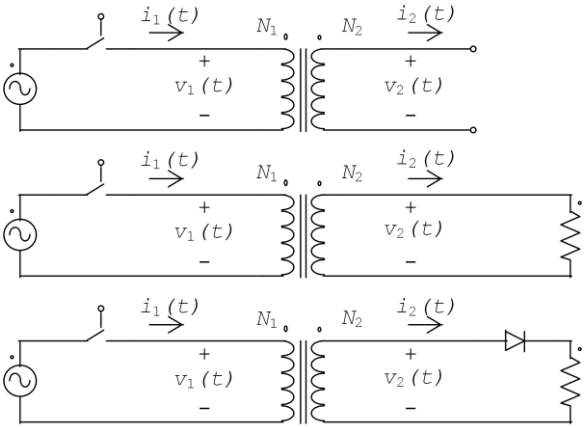

FIGURE 2. Load Types. Top: no-load; Middle: resistive load; Bottom: one-way rectifier with resistive load.

2) Ask the students what the expected primary current waveform for each case is, for a real transformer

During a brief discussion with the students, it is clear that some of them try to give a solution by using the ideal model, others are trying to explain the existence of magnetizing current and voltage drops with the T-linear model, and few are citing the current deformed by the magnetization curve, but almost no one manages to give consistent explanations for all models. After a brief period, typical experimental current waveforms are shown by the instructor to the students and a new round of discussions is held, allowing them to remake their hypotheses and explanations. It is a great opportunity to make clear for the students the need to review the concepts, reinforce them and learn new ones.

3) Ask students to experimentally measure the primary voltage $v_1(t)$ and current $i_1(t)$ for the 9 cases (three loads and three modes of operation)

This set of waveforms will be used throughout the 3 lectures and will be compared to those obtained via simulation in PSIM for the ideal, T-linear, and T-nonlinear models.

4) Present the conceptual electromagnetic model of Fig. 3, obtained from the real transformer

This model does not consider the core format and lamination, windings arrangement, shielding, cooling and other construction details. Along the three lectures, different simplifying hypotheses on the conceptual model led to three transformer physical electrical models: the ideal, T-linear and T-nonlinear ones.

5) Rescue of the hypotheses made to obtain the ideal model

The hypotheses made to obtain the ideal model are: a) core with infinite magnetic permeability μ, b) null core losses and null winding resistances, and c) perfect coupling i.e., the primary and secondary sides magnetic fluxes are the same, $\phi_1(t)=\phi_2(t)$ [7]. The focus is on the instantaneous behavior of electrical and magnetic variables, and not on their phasors.

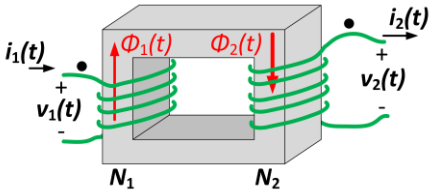

FIGURE 3. Conceptual electromagnetic model of the transformer.

From the analysis of electromagnetic phenomena of the conceptual model, and for no load condition at the transformer, students are remembered that

$$v_1(t) = N_1 \cdot d\phi_1(t)/dt\,, \tag{1}$$

where N_1 is the primary winding number of turns. By integrating (1)

$$\phi_1(t) = \phi_0(t) + (1/N_1)\int_{t_o}^{t} v_1(t)\,dt\,. \tag{2}$$

The primary flux density is given by (see Fig. 4 in blue)

$$B_1(t) = \phi_1(t)/S\,, \tag{3}$$

where S is the cross-sectional area of the core. Fig. 4 shows that for a sinusoidal $v_1(t)$, from the Faraday's law (1), the waveforms of the magnetic flux $\phi_1(t)$ (2), and of the flux density $B_1(t)$ (3) are both delayed by 90º with respect to $v_1(t)$.

The primary magnetic field $H_1(t)$ is calculated by (4). Since μ is infinite, $H_1(t)$ is null (see Fig. 4 in blue)

$$H_1(t) = B_1(t)/\mu = 0\,. \tag{4}$$

Based on Ampere's Law, $i_1(t)$ is also null (see Fig. 4 in blue)

$$H_1(t)l = N_1 i_1(t) \Rightarrow i_1(t) = 0\,, \tag{5}$$

where l is the core mean length.

Finally, applying Faraday's Law, remembering that $\phi_1=\phi_2$ and applying (1), the secondary voltage is (see Fig. 4 in blue)

$$\begin{aligned} v_2(t) &= N_2 \cdot d\phi_2(t)/dt = N_2 \cdot d\phi_1(t)/dt\,, \\ v_1(t)/v_2(t) &= N_1/N_2 = a\,, \end{aligned} \tag{6}$$

where N_2 is the secondary winding number of turns, and a is the turns ratio.

With the connection of a load at the secondary side, current circulates at the secondary winding. As $\phi_1=\phi_2$ and ϕ_1 is given by (1) and (2), considering that $v_1(t)$ is not modified, ϕ_2 cannot change even with the circulation of the secondary current. So, current must flow at the primary winding keeping equal magnetomotive forces at primary and secondary, i.e.,

$$i_1(t)N_1 = i_2(t)N_2 \Leftrightarrow i_1(t)/i_2(t) = N_2/N_1 = 1/a\,. \qquad (7)$$

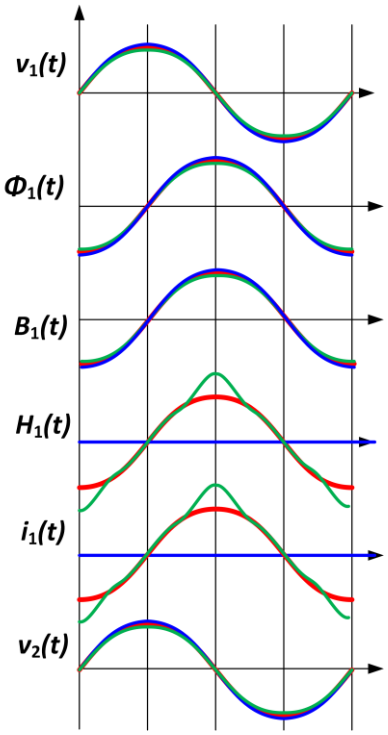

FIGURE 4. Typical waveforms for transformer models, no-load case. $v_1(t)$, $\phi_1(t)$, $B_1(t)$, $H_1(t)$, $i_1(t)$ and $v_2(t)$: ideal (blue), T-linear (red) and T-nonlinear (green) models.

The ideal electrical model given by (6) and (7) is represented in Fig. 5.

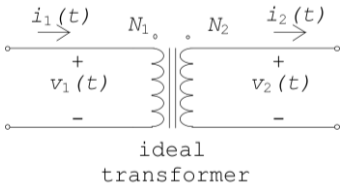

FIGURE 5. Ideal electrical transformer model.

It is important to emphasize to students that according to this model, $v_1(t) = a \cdot v_2(t)$ and $i_1(t) = i_2(t)/a$, from (6) and (7), even if $v_1(t)$ is pure DC voltage or a waveform with mean value. Moreover, (6) and (7) show that in the ideal transformer voltages and currents act independently from each other.

6) Simulation of the transformer with the ideal model (not shown in this paper)

Verification that the ideal model cannot represent the transient operation, nor the voltage drops, nor the deformation of the primary current (see related discussion in section IV).

B. *2nd LECTURE: T-LINEAR TRANSFORMER MODEL*

1) Recalling the hypotheses made to obtain the T-linear model

The hypotheses made to obtain the T-linear model are: a) μ with finite and constant value, b) inclusion of the iron and copper losses, and c) inclusion of the leakage flux [7]. Authors initially consider μ with finite and constant value, null copper and iron losses, no leakage flux and no-load operation, to sequentially obtain, for a sinusoidal $v_1(t)$, the waveforms of the magnetic flux by (2) and the flux density by (3), both delayed by 90° with respect to $v_1(t)$, as shown in Fig. 4 in red. Since the permeability is constant, the primary side magnetic field intensity is (see Fig. 4 in red)

$$H_1(t) = B_1(t)/\mu\,, \qquad (8)$$

and by Ampere's law (see Fig. 4 in red)

$$i_1(t) = H_1(t)l/N_1\,. \qquad (9)$$

It is important to notice that even with $i_2(t)=0$, there is a current in the primary side given by (9), what suggests a parallel branch. Constant μ in (8) results in sinusoidal magnetic field $H_1(t)$ and magnetizing current $i_1(t)$, both in phase with $B_1(t)$ and in quadrature with $v_1(t)$, explaining the inductive behavior of the magnetizing current. The constant magnetizing inductance L_m can be derived by substituting (3), (8) and (9) into (1), resulting in

$$v_1(t) = [N_1^2 S/(\mu l)] \cdot di_1(t)/dt = L_m\, di_1(t)/dt\,. \qquad (10)$$

Connecting a load at the secondary side results in secondary current, reflected to the primary as i_2' (Fig. 6). The ideal transformer model is complemented by the inclusion of R_m to model the core losses, R_1, R_2 to model the copper losses and L_1, L_2 to model the leakage fluxes (Fig. 6) [7]. It is important to emphasize again that an electromagnetic component is modeled by an equivalent electrical model.

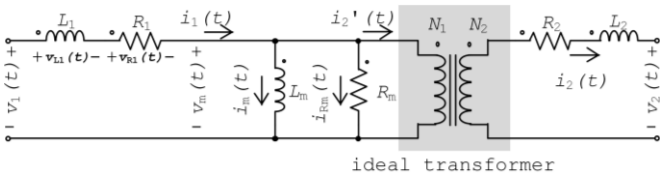

FIGURE 6. T-linear electrical transformer model.

2) No-load and short-circuit tests for the determination of T-linear model parameters, considering measured and MATLAB post processed instantaneous voltages and currents, and their waveform distortion

Here, students must pay attention for the non-sinusoidal characteristic of the no-load current, and the sinusoidal behavior of the short-circuit current. Students are asked to explain the waveforms and to discuss the validity of the usual no-load and short-circuit test procedures, based on rms

currents. Authors use the fundamental components of the measured currents and voltages for the tests, obtained by post processing these signals in MATLAB, similarly to the method presented in [15], as detailed in Appendix A.

3) Mathematical proof of important relations for transformers operating in steady state

Three important relations for transformers are mathematically proven during the lecture:

a) the average voltage in the leakage and magnetizing inductances is zero [7]. The inductor voltage is

$$v(t) = L\, di(t)/dt\,. \tag{11}$$

Considering an initial instant t_0, the inductor current after one period T is

$$i(t_0 + T) = (1/L)\int_{t_0}^{t_0+T} v(t)\cdot dt + i(t_0)\,. \tag{12}$$

Since in steady-state $i(t_0+T) = i(t_0)$, then it is demonstrated that the average voltage in an inductor V_{L_avg} is zero, i.e.,

$$(1/L)\int_{t_0}^{t_0+T} v(t)\cdot dt = (1/L)\cdot V_{L\_avg} = 0. \tag{13}$$

b) the average current on the primary side is zero [23] [24]. Applying Kirchoff's Law for the voltages in the primary side of Fig. 6 results in

$$v_1(t) = v_{L1}(t) + v_{R1}(t) + v_m(t)\,, \tag{14}$$

where v_{L1}, v_{R1} and v_m are the voltages over L_1, R_1 and L_m, respectively. Obtaining the average values of voltages over one period T in (14), remembering that v_1 is a sinusoidal voltage (i.e. null average value), and applying the result obtained in (13) for v_{L1} and v_m leads to

$$\frac{1}{T}\int_{t_0}^{t_0+T} v_{R1}(t)\cdot dt = V_{R1\_avg} = 0\,, \tag{15}$$

where V_{R1_avg} is the average voltage over R_1. From (15), equation (16) demonstrates that in steady state the average current in the primary I_{1_avg} is zero,

$$V_{R1\_avg} = \frac{R_1}{T}\int_{t_0}^{t_0+T} i_1(t)\cdot dt = R_1\cdot I_{1\_avg} = 0 \Rightarrow \quad I_{1\_avg} = 0. \tag{16}$$

c) the average value of the magnetizing current is equal to the average current reflected from the secondary with changed sign [23] [24]. Applying Kirchoff's Law for the currents in the primary side of Fig. 6 results in

$$i_1(t) = i_m(t) + i_{R_m}(t) + i_2'(t)\,, \tag{17}$$

where i_m, i_{Rm} and i_2' are the magnetizing, R_m and the reflected secondary currents. Obtaining the average values of the currents over one period T in (17), applying (16) for i_1, and applying (13) for the voltage over R_m (which is equal to voltage over L_m), then the average value of the magnetizing current I_{m_avg} is

$$0 = \frac{1}{T}\int_{t_0}^{t_0+T} i_m(t)\cdot dt + 0 + \frac{1}{T}\int_{t_0}^{t_0+T} i_2'(t)\cdot dt \Rightarrow \quad I_{m\_avg} = -I_{2\_avg}'. \tag{18}$$

4) Simulation of the 9 cases using the T-linear model and comparison with the experimental measurements made in the first lecture

Students verify that the T-linear model manages to adequately represent the voltage drops and losses for the operation of the 9 cases, and even the transient currents, although with significant error. However, it is unable to show the deformation in the primary current waveforms and the operation of the one-way rectifier. Some simulation and experimental results are shown and discussed in section IV.

5) Influence of the grid connection instant of transformer on its inrush current, for the linear model, and its validation through simulation and experiments

Students are expected to have learned how to calculate the transient behavior of series *RL* linear circuits under sinusoidal excitation, and to know that for a low loss inductor: a) the worst inrush current (nearly twice the steady state peak current) occurs if the *RL* is connected when the input voltage amplitude is approximately null; b) steady state is reached after about four-time constants (*4L/R*); c) small transient occurs for connection near the peak of the input voltage.

Authors consider important for engineers to do quick estimations based on simplified models. Therefore, considering only the magnetizing inductance L_m ($R_1 = 0$ and $R_m \to \infty$), for the no-load operation, fed by a sinusoidal voltage $v_1 = V_p \sin(\omega t)$ leads to (19) and (20)

$$v_m(t) = v_1(t) = L_m\, di_m(t)/dt\,, \tag{19}$$

$$i_m(t) = i_m(t_0) + 1/L_m\int_{t_0}^{t} V_p\, sin(\,\omega t)\, dt\,. \tag{20}$$

The connection at $t_0 = 0$, imposes positive voltage at L_m during all the first half cycle ($T/2$), producing a positive current excursion of $2V_p/(\omega L_m)$, that is twice the peak steady state expected current for a linear inductor, but lower than the current in a real transformer, as it is discussed in section III-C-5. In contrast, connection at $t_0 = T/4$ imposes positive voltage (increasing current) during only a quarter of cycle, resulting in a peak current of $V_p/(\omega L_m)$ at $t = T/2$, followed by a negative voltage that imposes a decreasing current. No transient is observed. It is important to emphasize to the students that the connection of the pure *L* circuit with initial conditions $v_m(0) = v_1(0) = \pm V_p$ and $i_m(0) = 0$, results in transient-less operation.

To consider the lossy operation, (21) and (22) include the series resistance R_1 that affects the inductor voltage $v_m(t)$ according to

$$v_m(t) = v_1(t) - R_1\cdot i_m = L_m\, di_m(t)/dt\,, \tag{21}$$

$$i_m(t) = i_m(t_0) + 1/L_m\int_{t_0}^{t}\left[V_p\, sin(\,\omega t) - R_1 i_m(t)\right] dt. \tag{22}$$

The increasing current behavior when connecting at $t_0=0$, reduces v_m amplitude during the first half cycle, forcing $i_1(t)$ to be always lower than the one in the no loss case. In the next half cycle, the still positive current decreases v_m, that will continue pushing $i_1(t)$ down until its average value becomes zero, when steady state is reached. Higher R_1 values increase the voltage drop ($R_1 \cdot i_m$), accelerating the decaying of the exponential component, as expected. Students can be remembered that theoretically, the no transient condition is achieved if the connection occurs at the instant corresponding to the electrical angle that is equal to the impedance angle.

Here, the transients were explained based on the electrical models. Depending on the available time, the discussion can also be carried out based on the electromagnetic model, emphasizing the behavior of ϕ_1, B_1 and H_1. Real nonlinear case is discussed in the next section.

C. 3rd LECTURE: T-NONLINEAR MODEL

1) Description of what happens when a nonlinear magnetization curve is considered, distorting the current and significantly increasing the inrush currents

Here the waveforms of $\phi_1(t)$, $B_1(t)$, $H_1(t)$ and $i_1(t)$ described in section III-B-1 are recalled, and the effect of a nonlinear B x H curve is discussed for the calculation of H_1. It is shown that in the saturated region, small increments of B_1 cause high excursion in H_1, and in the magnetizing current, distorting them as shown in green in Fig. 4. Also, the formula for L_m obtained in section III-B-1, shows that L_m can be considered as an inductor whose inductance depends on the value of the incremental magnetic permeability $\mu(t)$ defined by

$$B_1(t) = \mu(t) \cdot H_1(t) \,. \tag{23}$$

The permeability $\mu(t)$ varies with $H_1(t)$, i.e., with $i_m(t)$. As a result, the nonlinear model substitutes the fixed magnetizing inductance of the T-linear model by a variable inductance $L_m(i_m)$ to model the effect of core saturation, resulting in Fig. 7, where

$$v_m(t) = L_m(i_m) \cdot di_m(t)/dt \,. \tag{24}$$

This nonlinear behavior can be seen in Fig. 4 (in green) for the waveforms of $H_1(t)$ and $i_1(t)$, when a sinusoidal primary voltage is applied for the no-load, no leakage flux and no losses condition.

2) Presentation of a T-nonlinear model

The magnetizing inductance L_m is exchanged by an inductor whose inductance varies with the current (see Fig. 7).

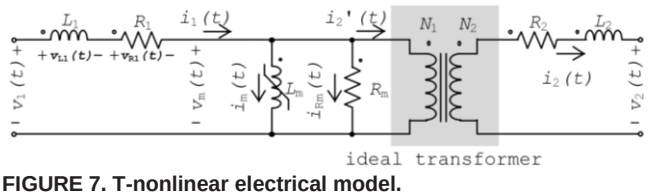

FIGURE 7. T-nonlinear electrical model.

3) Show a possible model for the nonlinear saturable inductor L_m

In this model (see fig. 8) [15] the voltage v_m across L_m is integrated, producing the concatenated flux $N_1\phi_1$, which is applied to a Math Function block, resulting in the current i_m that will be imposed by a controlled current source. This saturable inductor model is adopted in the lectures and implemented in PSIM. The reason why the $N_1\phi_1$ x i_m curve instead of the B x H curve is used in this paper is discussed in Appendix B.

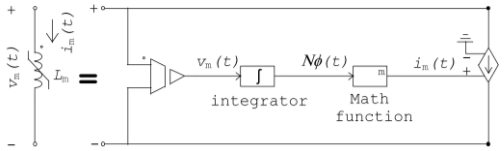

FIGURE 8. Saturable inductor model.

Another possible model of a saturable inductor, which consists of parallel association of switched inductors, is also discussed in the lecture. This approach is based on approximating the $N_1\phi_1$ x i_m curve of Fig. 9 by several lines with different slopes, and it is denominated as local linearization or discontinuous method [15].

4) The Math Function in Fig. 8 can be obtained from the saturation curve, that must adequately represent the region with strong saturation

Transient measurements of $v_1(t)$ and $i_1(t)$ are used with no load at the secondary side [15] [25], switched at $\theta=0^o$, which are processed numerically to obtain the Math Function (current i_m as a function of concatenated flux $N_1\phi_1$), following the steps next described. The voltage $v_m(t)$ at L_m is numerically calculated [15] by subtracting the voltage drop across R_1 and L_1 from $v_1(t)$ and integrated to obtain $N_1\phi_1$. The current i_m at L_m is numerically calculated by subtracting the current across R_m, i.e., $v_m(t)/R_m$ from $i_1(t)$. The objective is to obtain the saturation curve instead of the hysteresis loop, since the core losses are not considered in L_m [26].

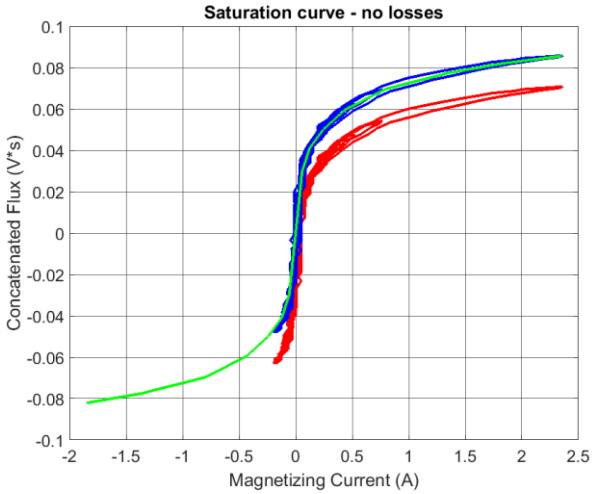

FIGURE 9. Saturation curve ($N_1\phi_1$ x i_m). a-red: original curve; b-blue: vertical offset corrected curve; c-green: resulting fitted curve.

The $N_1\phi_1$ x i_m curve (Fig. 9a) will be vertically displaced by the residual concatenated flux $\Delta N_1\phi_1$, that depends on the current behavior prior to the disconnection of the transformer from the AC source. Instead of numerically correcting the

vertical offset and adjusting data by curve fitting, as it is done in [15], authors propose students to visually displace the original curve with the help of MATLAB, by adding a $\Delta N_1\phi_1$ of approximately -0.02 V*s in Fig. 9a (red) to all concatenated flux points, obtaining Fig. 9b (blue). Next, a set of curve coordinates (i_m, $N_1\phi_1$) is collected in the first quadrant by using the GINPUT function of MATLAB. The third quadrant is constructed by mirroring the first quadrant (Fig. 9c, green), generating the i_m x $N_1\phi_1$ curve, and the collected data is saved in a *.txt* file that will be used to implement the 'Math Function' in Fig. 8 by means of a 'Lookup Table' PSIM block.

5) Discussion of the influence of the connection angle on the high amplitude inrush for the nonlinear case

Considering the equivalent nonlinear circuit model, the connection at $t=0$, will saturate L_m producing currents higher than twice the steady state peak currents. Taking into account that: a) the transformer is designed to operate with a peak flux density $B_1=B_{1max}$ near the knee of the magnetization curve and b) that the connection at $t=0$ imposes $B_1=2B_{1max}$, high inrush currents will occur due to strong core saturation.

6) Simulation of the T-nonlinear model and comparison with the experimental values

It is shown that the T-nonlinear model is adequate to represent the high inrush currents and the current distortion, even for the one-way rectifier (see simulation and experimental results, and related discussion in section IV).

IV. A SET OF RESULTS

The presentation of the results in this section does not follow the step-by-step procedure along the three lectures, as this is inadequate for a paper. Also, it does not show the complete set of results due to lack of space. The main objective is to show and comparatively discuss what authors consider to be the most important results to be pointed out for the students.
Experimental and simulation results are presented in Figs. 10 to 13 for different loads and energization instants. Simulation parameters are presented in Table I, obtained according to the tests of Appendix A.

TABLE I. Transformer Simulation Parameters.

R_1, R_2	2.04 Ω
L_1, L_2	0.0909 mH
R_m	362 Ω
L_m	0.323 mH
a	1

Experimental results, simulation of the T-linear model and simulation of the T-nonlinear model are respectively shown at the top, center and bottom of Figs. 10 to 13. In these figures, one cycle of steady state operation is presented in a small zoom window near each transient waveform. Although it is expected by the reader, primary voltage v_1 is not displayed in large figures to avoid impairing readability. Even so, energizing instant can be easily noticed in the figures. Also, for readability and for easy comparison with simulated results, prints of the oscilloscope screen were avoided, and thus experimental results were plotted using MATLAB. Simulated waveforms using PSIM are shown only for the T-linear and T-nonlinear, but the ideal model is requested for students, for a complete analysis. For improved readability, PSIM simulation waveforms are also plotted by using MATLAB.

Fig. 10 shows the primary current $i_1(t)$ for the no-load case. Only the energization at the zero crossing of grid voltage ($\theta=0°$) is shown in Figs. 10 and 11. However, authors consider it very important for the students to confirm the no transient energization ($\theta=90°$) in the lectures. The fact that the flux density reaches a value approximately twice its value in steady state in the first cycle after energization at $\theta=0°$, generates in the linear case (Fig. 10b) an inrush current of almost twice the nominal current, as explained in section III-B-5. In the real case (Fig. 10a), the saturation of the B x H curve causes high amplitude inrush currents, which are adequately represented only by the T-nonlinear model (Fig. 10c).

Considering the resistive full load case, the T-linear model (Fig. 11b) is adequate for describing the operation at steady state (Fig. 11a), but it cannot describe the initial transient current, as the T-nonlinear model can do (Fig. 11c).

Considering the one-way rectifier, T-linear model (Fig. 12b) is not able to adequately describe neither the initial transient nor the steady state current (Fig. 12a). It is important to notice that for the one-way rectifier load [23] [24]:

i) Primary current present high negative peaks in steady state (Fig. 12a), even considering that the secondary current is always positive. There is a transient in the behavior of the negative peaks (Fig. 12a), produced by the magnetizing current. The steady state is reached when the average value of the magnetizing current is equal to the negative average value of the reflected secondary current, as stated by (18). This results in a primary current with null average value at steady state, as predicted by (16), that can be noticed in the experimental and simulated waveforms of Fig. 12. Both linear (Fig. 12b) and nonlinear (Fig. 12c) models show the initial positive and negative transients, but the discrepancies in the first case are high when compared to the experimental waveforms (Fig. 12a);

ii) The increasingly negative magnetizing current (Fig. 12a) is explained by the voltage drop at R_1, that occurs only at the positive semi cycles, producing a voltage v_m with negative locally averaged value at the first cycles. It causes a monotonically decreasing behavior in the locally averaged value of flux density that will force the asymmetrical operation in the saturation curve, causing high amplitude negative peak current even at steady state;

iii) For connection at $\theta=90°$ (Fig. 13a) the initial positive transient is absent, but the negative transient still exists. Again, the T-nonlinear model (Fig. 13c) presents a better performance than the linear one (Fig. 13b). The steady state waveforms are the same as shown in Fig. 12, and thus they are not presented in Fig. 13.

Figs. 14 and 15 show simulation results of the T-linear and nonlinear models with the one-way rectifier and resistive load, for $\theta=0°$ and $\theta=90°$, using Table I parameters. It clarifies understanding of the waveform of the primary currents as the sum of the magnetizing (blue) and secondary reflected current (red). The secondary current is the typical waveform of this load. For the linear model, i_m is sinusoidal (Fig. 14a top) since saturation is not considered. When the nonlinear L_m is adopted, i_m is distorted as it can be seen in the top of Fig. 15a. In both Figs. 14 and 15, the waveform of i_1 can be explained by summing i_m and the reflected secondary current i_2' waveforms [23] [24], and by applying the results

of (13), (16) and (18), thus complementing the previous analysis of Figs. 12 and 13.

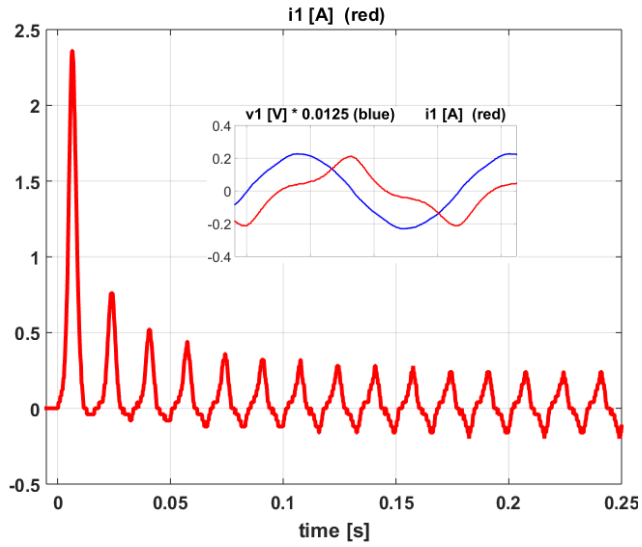

(a) experimental.

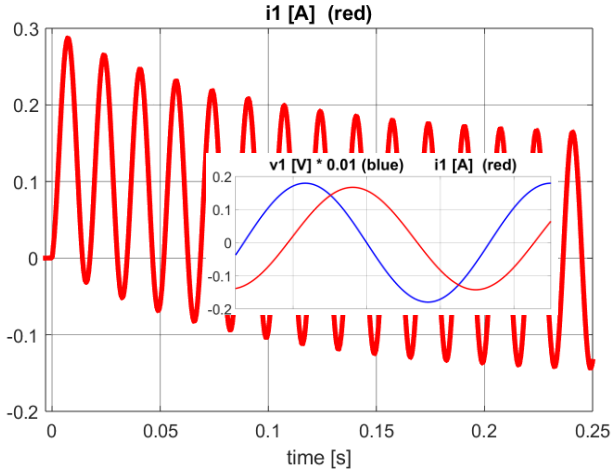

(b) simulation using T-Linear model.

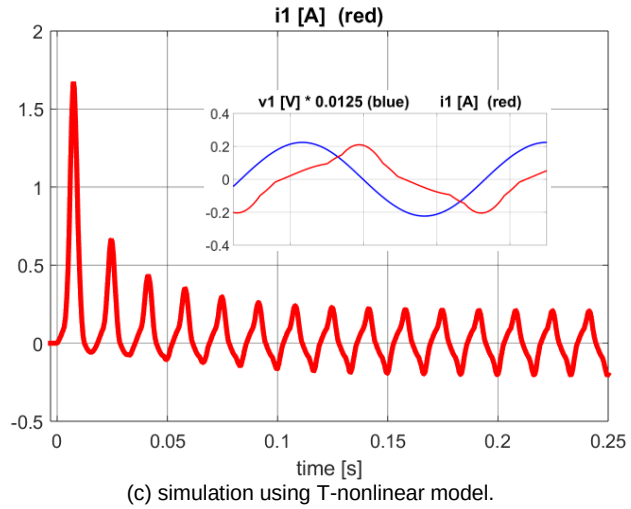

(c) simulation using T-nonlinear model.

FIGURE 10. No-load waveforms. Primary current i_1 transient for connection at $\theta=0^o$. Small figure: v_1 and i_1 for steady state operation.

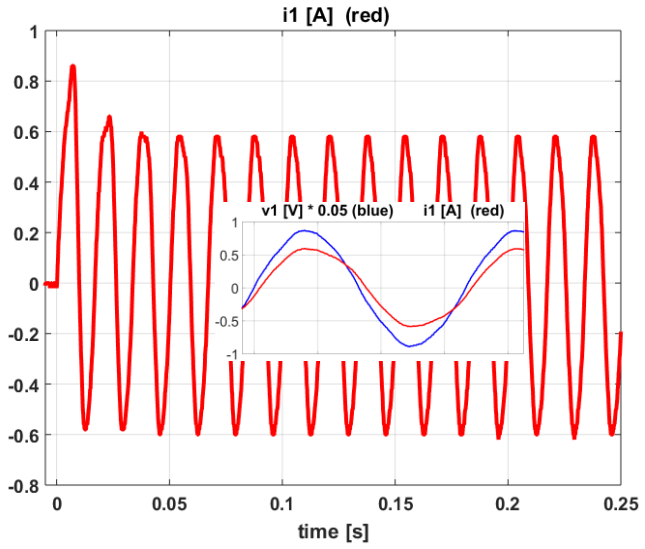

(a) experimental.

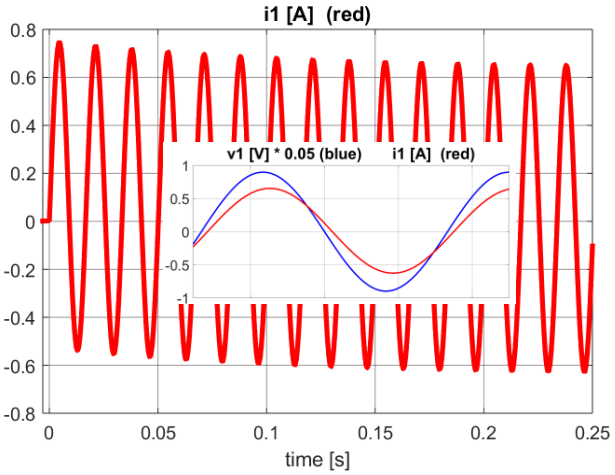

(b) simulation using T-Linear model.

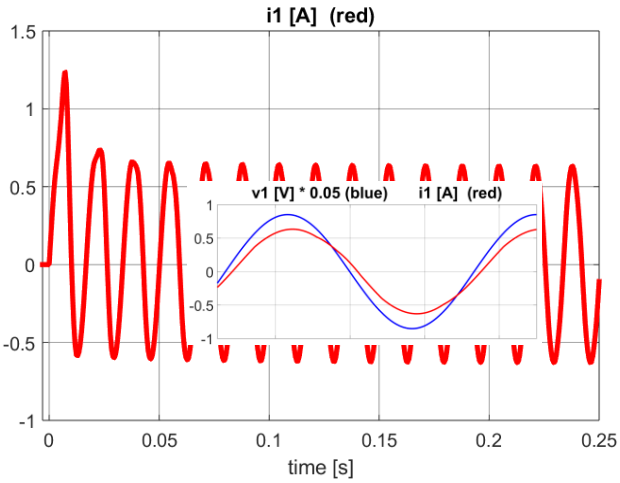

(c) simulation using T-nonlinear model.

FIGURE 11. Resistive load waveforms. Primary current i_1 transient for connection at $\theta=0^o$. Small figure: v_1 and i_1 for steady state operation.

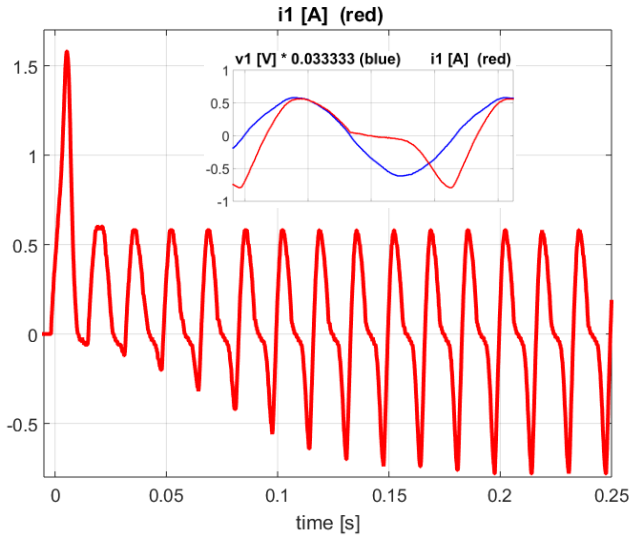

(a) experimental.

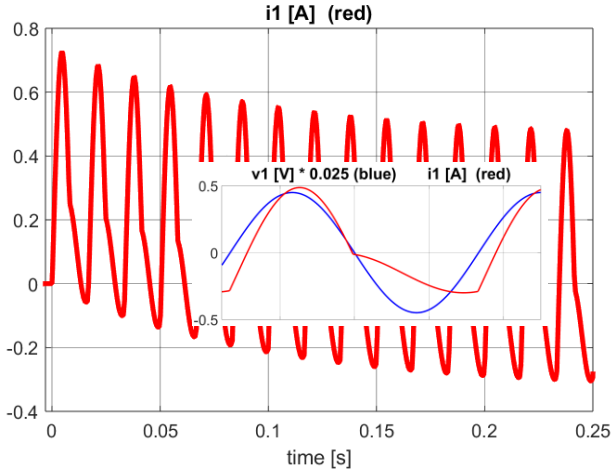

(b) simulation using T-Linear model.

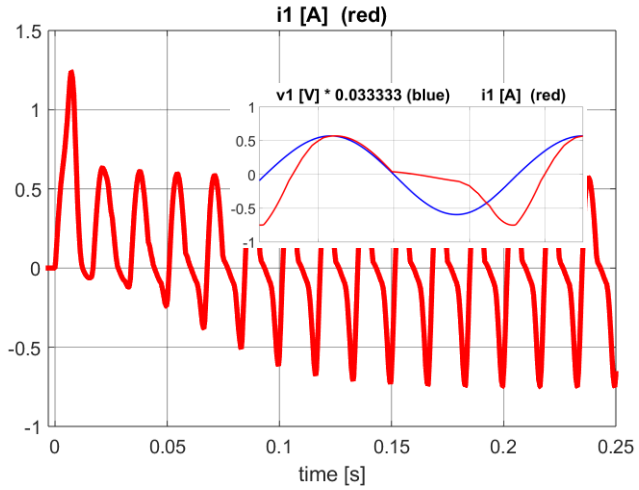

(c) simulation using T-nonlinear model.

FIGURE 12. Primary current i_1 transient for one-way rectifier with resistive load for connection at $\theta=0^o$. Small figure: v_1 and i_1 for steady state operation.

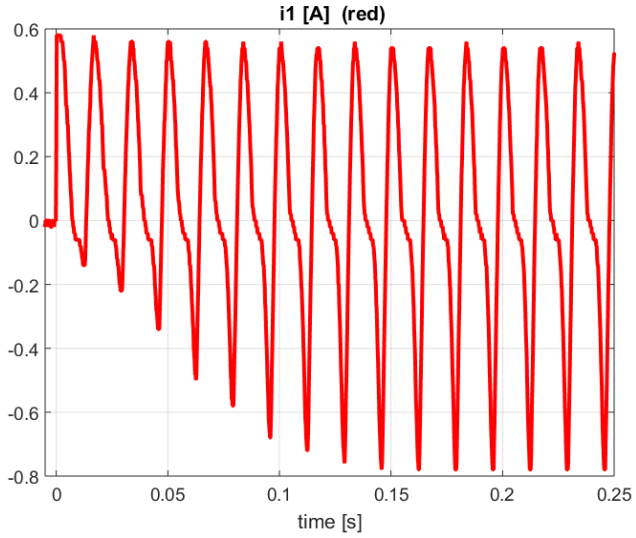

(a) experimental.

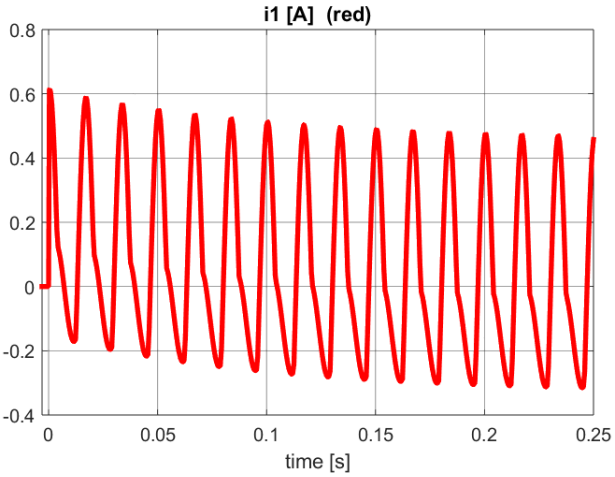

(b) simulation using T-Linear model.

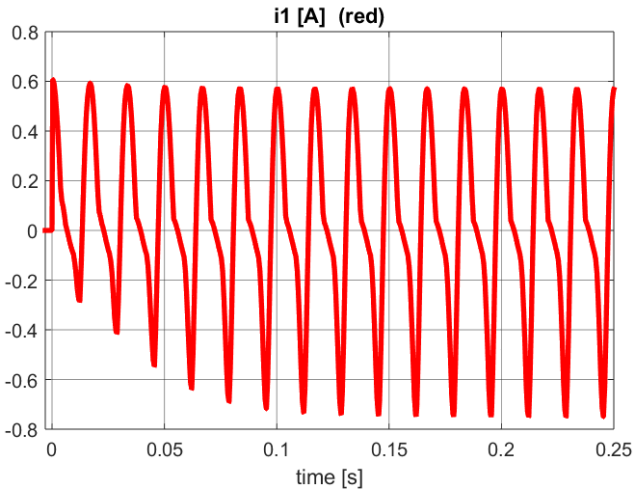

(c) simulation using T-nonlinear model.

FIGURE 13. Primary current i_1 transient for one-way rectifier with resistive load for connection at $\theta=90^o$.

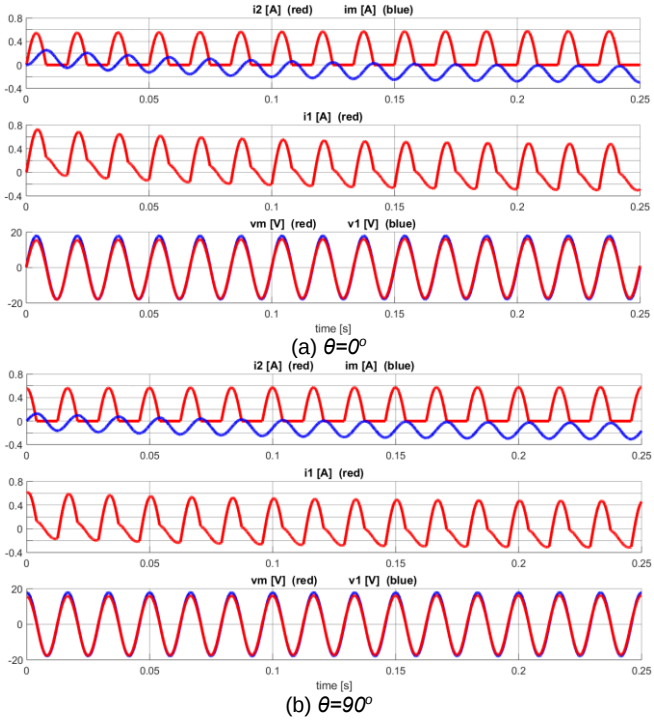

(a) $\theta=0^o$

(b) $\theta=90^o$

FIGURE 14. Simulation of T-Linear model for the one-way rectifier with resistive load, when $\theta=0^o$ and $\theta=90^o$. Top: secondary (i_2) and magnetizing (i_m) currents. Middle: primary current (i_1). Bottom: magnetizing (v_m) and primary voltages (v_1).

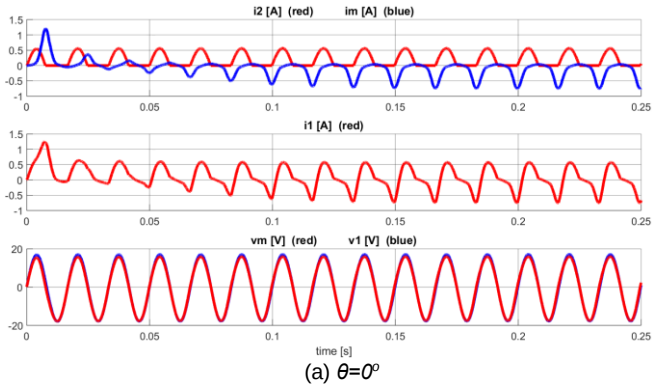

(a) $\theta=0^o$

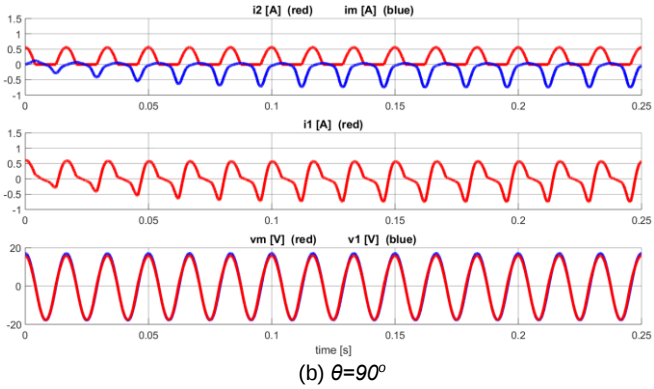

(b) $\theta=90^o$

FIGURE 15. Simulation of T-nonlinear model for the one-way rectifier with resistive load, when $\theta=0^o$ and $\theta=90^o$. Top: secondary (i_2) and magnetizing (i_m) currents. Middle: primary current (i_1). Bottom: magnetizing (v_m) and primary voltages (v_1).

The T-nonlinear model accurately describes all the considered operation modes, except for the initial positive transient (Figs. 10a and 10c; Figs. 11a and 11c; Figs. 12a and 12c), that is defined by the primary voltage source and depends on the residual flux [15] [25].

The compensation of the residual flux on the modeling of the nonlinear inductor, based on experimental tests, was adequately solved in section III-C-4. Unfortunately, correct simulation results with the T-nonlinear model would require the knowledge of the residual flux value previously to the connection of the transformer, which is unknown, or the demagnetization of the transformer before carrying out any transient acquisition [26] [27], and would require the use of a trigger circuit to guarantee the energization of the transformer at the desired grid voltage angle.

Concluding, lecturers emphasize to the students that there is no complete model, and that model improvements are always possible, at the expense of obtaining additional parameters and of increasing complexity.

V. METHODOLOGY EVALUATION

These lectures have been taught in 2022 and 2023 for a total of 54 students. Students were asked by means of an online questionnaire about the learning methodology adopted in the PE courses. As a result, 51.9% of the students answered that this is a good methodology and should not be changed for future PE courses, and 48.1% answered that the methodology is good but must be improved for future courses. The other options, with no answers were: 'It is a bad strategy. It is better to return to conventional lectures'; 'I don't consider PE necessary for my professional career'.

When asked if the theory and experiment classes on transformers modeling were an opportunity to review or consolidate concepts and to learn new subjects, 81.5% of students rated it 4 or 5, and 7.4% rated it 3, with 0 being totally disagree and 5 being totally agree. Additionally, 11.1% did not attend these lectures for different reasons.

When asked if they felt motivated by theory and experiment classes on transformers modeling, 63.0% of students rated it 4 or 5, and 25.9% rated it 3, with 0 being totally disagree and 5 being totally agree. Additionally, 11.1% did not attend these lectures for different reasons.

VI. CONCLUSION

These three lectures of a Power Electronics course were an opportunity for students to learn about the whole process of developing and improving the model of one component/system. The single-phase transformer was chosen because it was already known by the students, and it is used in many power electronics topologies. Students were able to review and consolidate concepts of electrical circuits, measurements and energy conversion, including the hypotheses adopted to obtain the ideal and T-linear transformer models, as well as the experimental tests for obtaining their parameters. After verifying the limitations of these models to describe the behavior of three selected test circuits, in particular for a one-way rectifier, an improved T-nonlinear model was developed, together with one method for parameter estimation. This nonlinear model has adequately described the behavior of the nine test cases.

Authors consider this set of three lectures about transformer modeling enough for this PE undergraduate course, but there are still many topics to be explored in a more advanced course on transformers modeling, like: i) how to take into account the residual flux during the parameter determination step; ii) how to estimate the residual flux for a given transformer, prior to the test; iii) methods and adequate functions to be

used for saturation curve fitting; iv) operation at high frequency and modeling of the parasitic capacitances, etc.

Finally, it must be highlighted that the use of this teaching methodology can be also adequate for a course on System Modeling.

APPENDIX A. OPEN AND SHORT CIRCUIT TEST METHODS

Open and short circuit tests are done to obtain the T-linear model parameters, using a variable source and an oscilloscope to acquire voltage and currents, similarly to the method presented in [15]. The grid frequency is 60Hz.

In the open circuit test, the low voltage (primary) side is fed with nominal voltage and the high voltage side is left opened. The primary and secondary windings resistances and leakage inductances are neglected. The objective of the test is to calculate L_m, R_m and the turns ratio N_1/N_2.

After acquiring one cycle of the primary side voltage and current, a MATLAB routine is performed to calculate the active power P_{OC}, the rms voltage V_{rms}, the fundamental component of the primary voltage V_{1rms_OC} and the fundamental component of the primary current I_{1rms_OC}. Considering that all active power is consumed by R_m, then

$$R_m = (V_{1rms\_OC})^2/P_{OC}\ . \tag{A.1}$$

In the same way, all the fundamental reactive power is due to L_m

$$Q_{1\_OC} = \sqrt{(V_{1rms\_OC}I_{1rms\_OC})^2 - {P_{OC}}^2} \quad = \left(V_{1rms\_OC}^2/2\pi 60 L_m\right), \tag{A.2}$$

where Q_{1_OC} is the reactive power associated to the fundamental primary current component. Since the measured current and voltage are distorted, the MATLAB routine extracts the fundamental component (60Hz) to compute L_m, instead of using the rms values of the traditional method. Thus

$$L_m = V_{1rms\_OC}^2/\left(2\pi 60 \cdot Q_{1\_OC}\right). \tag{A.3}$$

The turns ratio is given by (6), where the primary and secondary voltages can be measured by using an oscilloscope or a multimeter.

In the short circuit test, the low voltage (primary) side is fed with reduced voltage by means of a variable voltage source, and the secondary side is short circuited. This voltage source must be carefully varied till the primary rated current is achieved. The parameters of the magnetizing branch are neglected. The objective of the test is to calculate the windings resistances R_1, R_2, and the leakage inductances L_1, L_2.

The total resistance and inductance referred to the primary side are

$$R = R_1 + a^2 R_2\ , \tag{A.4}$$

$$L = L_1 + a^2 L_2\ . \tag{A.5}$$

Acquiring again one cycle of the primary voltage and currents, the MATLAB routine calculates P_{SC}, V_{1rms_SC} and I_{1rms_SC}. Considering that all active power is consumed by R, then

$$R = P_{SC}/I_{1rms\_SC}^2. \tag{A.6}$$

In the same way, if all reactive power is due to L, then

$$Q_{1\_SC} = \sqrt{(V_{1rms\_SC}I_{1rms\_SC})^2 - {P_{SC}}^2} = I_{1rms\_SC}^2 2\pi 60 L\ ,$$
$$L = Q_{1\_SC}/\left(2\pi 60 \cdot I_{1rms\_SC}^2\right). \tag{A.7}$$

As stated in [12], approximated values of R_1 and R_2 can be obtained by assuming that

$$L_1 = a^2 L_2 = L/2\ , \tag{A.8}$$

$$R_1 = a^2 R_2 = R/2\ . \tag{A.9}$$

APPENDIX B. DISCUSSION ON THE USE OF $N_1\phi_1$ X I_M CURVE

As it was mentioned in section III.C-3, this paper uses the $N_1\phi_1$ x i_m curve instead of the B x H curve to obtain the nonlinear magnetizing inductance of the transformer. This topic briefly presents the reasons to adopt this methodology.

According to (10), the calculation of the magnetizing inductance depends on the knowledge of the primary side number of turns (N_1), the core cross sectional area (S), the permeability (μ) and of the magnetic path length (l). However, in practice neither the hysteresis curve of the core nor the previous parameters are available for the tests.

On the other hand, working with the $N_1\phi_1$ x i_m curve only requires acquisition of the instantaneous (primary) voltage and current of the transformer for the no-load condition. Thus, once $v_1(t)$ is measured, the concatenated flux is calculated by

$$N_1\phi_1 = \int v_1(t)dt\ . \tag{B.1}$$

Since $i_1(t)$ is also measured, it is possible to plot the curve $N_1\phi_1$(t) x i_1(t). As stated before, the slope of this curve is the magnetizing inductance if the winding and eddy losses are neglected (or subtracted as it is done in this paper), which is given by

$$L_m = N_1\phi_1/I_1\ . \tag{B.2}$$

In this way, by using this method, the magnetizing inductance may be determined without the knowledge of the magnetic circuit parameters.

I. ACKNOWLEDGMENT

This work was financially supported by the National Council for Scientific and Technological Development (CNPq) – undergraduate grant 120725/2022-3, and by Amigos da Poli Endowment (purchase of electronic components). This study was financed in part by the Coordenação de Aperfeiçoamento de Pessoal de Nível Superior – Brasil (CAPES) – Finance Code 001.

AUTHOR CONTRIBUTION

MACHADO, V.N.: Conceptualization, Data Curation, Formal Analysis, Investigation, Methodology, Software, Validation, Visualization, Writing – Review & Editing. **MARTINZ, F.O.**: Conceptualization, Data Curation, Formal Analysis, Investigation, Visualization, Writing – Original Draft, Writing – Review & Editing. **KOMATSU, W.**: Conceptualization, Formal Analysis, Funding Acquisition, Investigation, Methodology, Resources, Supervision, Writing – Review & Editing. **MATAKAS JUNIOR, L.**: Conceptualization, Formal Analysis, Funding Acquisition, Investigation, Methodology, Project Administration, Resources, Software, Supervision, Validation, Visualization, Writing – Original Draft, Writing – Review & Editing.

PLAGIARISM POLICY

This article was submitted to the similarity system providedby Crossref and powered by iThenticate – Similarity Check

REFERENCES

[1] H. L. S. Almeida, “Modelagem matemática de sistemas físicos [Mathematical modeling of physical systems]”, 2023, [Online], in Portuguese, available: http://del.ufrj.br/~heraldo/eel660_slides_04_Modelagem_Matematica_de_Sistemas_Fisicos.pdf .

[2] T. H. Sloane, "Laboratories for an undergraduate course in power electronics," *IEEE Trans. Education*, vol. 38, no. 4, pp. 365-369, Nov. 1995, doi: 10.1109/13.473158.

[3] J. A. Pomilio, “Atividades Didáticas Experimentais em Eletrônica de Potência: Convergindo Conhecimentos e Tecnologias [Experimental Activities in Power Electronics Course: Merging Knowledge and Application]*”,* in Portuguese, *Eletrônica de Potência*, vol. 25, no. 2, pp. 146–153, Jun. 2020, doi: 10.18618/REP.2020.2.0023.

[4] S. Lotfifard, “Teaching Electrical Model of Power Transformers to Undergraduate Students: Magnetic Circuit Approach” *Physics Education*, 2021, doi: 10.48550/arXiv.2103.17257.

[5] L. Matakas, V. N. Machado, F. O. Martinz and W. Komatsu, “Learning Transformer Modeling: A Laboratory Approach for Undergraduate Lectures”, *in Proc of SPEC/COBEP*, Florianopolis, Brazil, pp. 1-8, 2023, doi: 10.1109/SPEC56436.2023.10408680.

[6] D. W. Hart, *Introduction to Power Electronics*, Prentice Hall, 1st Edition, Upper Saddle River, 1997, pp. 236-262.

[7] N. Mohan, T.M. Undeland and W.P. Robbins, *Power Electronics: Converters, Applications, and Design*, John Wiley and Sons, 3rd Edition, New York, 2003, pp. 52-57, pp. 304-319.

[8] *IEEE Recommended Practice for Calculating AC Short-Circuit Currents in Industrial and Commercial Power Systems [The Violet Book]*, IEEE Std 551-2006, doi: 10.1109/IEEESTD.2006.248693.

[9] P. Kundur, *Power System Stability and Control*, 1st Edition, McGraw-Hill, Palo Alto, 1994, pp. 231-235.

[10] G. M. S. Azevedo, M. C. Cavalcanti, F. A. S. Neves, L. R. Limongi, and F. Bradaschia, “Microgrid Power Converter Control With Smooth Transient Response During the Change of Connection Mode”, *Eletrônica de Potência*, vol. 19, no. 3, pp. 285–294, Aug. 2014, doi 10.18618/REP.2014.3.285294.

[11] R. C. Dugan, M. F. McGranaghan, S. Santoso and H.W. Beaty, *Electrical Power Systems Quality*, 3rd Edition, US, McGraw-Hill Professional, 2012.

[12] A. E. Fitzgerald, C. Kingsley Jr. and S.D. Umans, *Electric Machinery*, McGraw-Hill, 5th Edition, New York, 1990, pp. 60-73.

[13] R. W. Ericksson and D. Maksimovic, *Fundamentals of Power Electronics*, 2nd Edition, Kluwer Academic Publishers, Norwell, 2001, pp. 146-170.

[14] W. M. dos Santos and D. C. Martins, “Introdução ao Conversor DAB Monofásico [Introduction to Single Phase DAB Converter]”, in Portuguese, *Eletrônica de Potência*, vol. 19, no. 1, pp. 36–46, Mar. 2014, doi: 10.18618/REP.2014.1.036046.

[15] T. C. Monteiro, F. O. Martinz, L. Matakas and W. Komatsu, "Transformer Operation at Deep Saturation: Model and Parameter Determination," *IEEE Trans. on Industry Applications*, vol. 48, no. 3, pp. 1054-1063, May-June 2012, doi: 10.1109/TIA.2012.2190256.

[16] S. Hodder, B. Kasztenny, N. Fischer and Y. Xia, "Low second-harmonic content in transformer inrush currents - Analysis and practical solutions for protection security," *in Proc. of CPFR*, TX, USA, 2014, pp. 705-722, doi: 10.1109/CPRE.2014.6799037.

[17] K. Subramanya, T. R. Chelliah, “DC bias impact analysis on the capability of power transformer and failure risks”, *Engineering Failure Analysis*, vol. 163, part B, 108537, 2024, doi: 10.1016/j.engfailanal.2024.108537.

[18] D. A. Fernandes, F. F. Costa, J. D. Inocêncio, A. C. Castro, I. S.de Freitas, "Dynamic Voltage Restorer with Complete Control of the Connection Transformers Saturation" in *Eletrônica de Potência*, vol. 18, no. 3, pp. 1030–1037, Aug. 2013, doi: 10.18618/REP.2013.3.10301037.

[19] S. S. H. Bukhari and J. Ro, "A Single-Phase Line-Interactive UPS System for Transformer-Coupled Loading Conditions," in *IEEE Access*, vol. 8, pp. 23143-23153, 2020, doi: 10.1109/ACCESS.2020.2970489.

[20] T. Nakajima, K. -I. Suzuki, M. Yajima, N. Kawakami, K. -I. Tanomura and S. Irokawa, "A new control method preventing transformer DC magnetization for voltage source self-commutated converters," in *IEEE Trans. on Power Delivery*, vol. 11, no. 3, pp. 1522-1528, July 1996, doi: 10.1109/61.517512.

[21] L. Koleff et al., "Development of a Modular Open-Source Power Electronics Didactic Platform," *in Proc. of COBEP/SPEC*, Santos, Brazil, pp. 1-6, 2019, doi: 10.1109/COBEP/SPEC44138.2019.9065327.

[22] *Audio/video, information and communication technology equipment - Part 1: Safety requirements*, IEC 62368-1:2023, 2023.

[23] E. A. C. Lourenço, W. Komatsu, and L. Matakas Junior, “A common error in the determination of AC primary transformer current waveforms in one-way half-wave rectifiers”, *in Proc. of IPEC*, Niigata, Japan, 2005.

[24] H. Von Bertele and H. Grasl, “Anomalies in Converter Transformer Operation”, *Direct Current*, London, p. 203-214. Aug. 1962.

[25] S. Bogarra, A. Font, I. Candela and J. Pedra, “Parameter estimation of a transformer with saturation using inrush measurements”, *Electric Power Systems Research*, vol. 79, no. 2, pp. 417-425, Feb. 2009, doi: 10.1016/j.epsr.2008.08.009.

[26] J. L. Velásquez, K. Vennemann, P. Wischtukat, “On-site measurement of the hysteresis curve for improved modelling of transformers”, *Electric Power Systems Research*, vol. 223, 109661, 2023, doi: 10.1016/j.epsr.2023.109661.

[27] L. F. Blume, G. Camilli, S. B. Farnham and H. A. Peterson, "Transformer magnetizing inrush currents and influence on system operation," *Electrical Engineering*, vol. 63, no. 6, pp. 366-374, June 1944, doi: 10.1109/EE.1944.6440312.

BIOGRAPHIES

Vinicius Negri Machado born in 18/07/2001 in São Paulo, Brazil, received the B.S. degree in electrical engineering (2023) from the Polytechnic School of the University of São Paulo (EPUSP), São Paulo, where he is currently working towards the M.S degree. His areas of interest are: power electronics, power quality, electronic control systems, grid-connected power converters modeling and control, and grid-forming converters. Mr. Machado is a student member of the Brazilian Power Electronics Society (SOBRAEP).

Fernando Ortiz Martinz received the B.S. degree in electrical engineering from the State University of Campinas, São Paulo, Brazil, in 2003, and the M.S. and Ph.D. degrees from the Polytechnic School of the University of São Paulo (EPUSP), São Paulo, Brazil, in 2007 and 2013, respectively. His interests are: modeling, control, and synchronization in power electronics, power quality, and grid-connected power converters. Dr. Martinz is a member of the Brazilian Power Electronics Society (SOBRAEP).

Wilson Komatsu born in São Paulo, Brazil, in 1963. He received the B.S., M.S., and Ph.D. degrees in electrical engineering from the Polytechnic School of the University of São Paulo (EPUSP), São Paulo, in 1986, 1992, and 2000, respectively. He is an Associate Professor of power electronics at EPUSP. His research areas are control and modeling of static converters, and their application to electrical power systems and electrical power quality. Dr. Komatsu is a member of the Institute of Electrical and Electronics Engineers (IEEE) and of the Brazilian Power Electronics Society (SOBRAEP).

Lourenco Matakas Junior received the B.S., M.S., and Ph.D. degrees in electrical engineering from the Polytechnic School of the University of São Paulo (EPUSP), Sao Paulo, in 1984, 1989, and 1998. He is an Associate Professor at EPUSP. His research focuses on topologies, control and application of static converters connected to the grid, phase-locked loops, and pulse width modulation strategies. He is a member of the Brazilian Power Electronics Society (SOBRAEP) and of the Institute of Electrical and Electronics Engineers (IEEE).